HHS Public Access

Author manuscript

Nat Med. Author manuscript; available in PMC 2013 September 01.

Published in final edited form as:

Nat Med. 2013 March ; 19(3): 295–304. doi:10.1038/nm.3070.

Epidermal Growth Factor Regulates Hematopoietic Regeneration Following Radiation Injury

Phuong L. Doan[1], **Heather A. Himburg**[1], **Katherine Helms**[1], **J. Lauren Russell**[1], **Emma Fixsen**[1], **Mamle Quarmyne**[4], **Jeffrey R. Harris**[1], **Divino Deoliviera**[1], **Julie M. Sullivan**[2], **Nelson J. Chao**[1,3], **David G. Kirsch**[2,4], and **John P. Chute**[1,4]

[1]Division of Hematologic Malignancies and Cellular Therapy, Department of Medicine, Duke University, Durham, NC

[2]Department of Radiation Oncology, Duke University, Durham, NC

[3]Department of Immunology, Duke University, Durham, NC

[4]Department of Pharmacology and Cancer Biology, Duke University, Durham, NC

Abstract

The mechanisms which regulate HSC regeneration following myelosuppressive injury are not well understood. We identified epidermal growth factor (EGF) to be highly enriched in the bone marrow (BM) serum of mice bearing deletion of *Bak* and *Bax* in Tie2^{+} cells (*Tie2Cre;Bak1*$^{-/-}$*;Bax*$^{fl/-}$ *mice*), which displayed radioprotection of the HSC pool and 100% survival following lethal dose total body irradiation (TBI). BM HSCs from wild type mice expressed functional EGFR and systemic administration of EGF promoted the recovery of the HSC pool in vivo and the improved survival of mice following TBI. Conversely, administration of erlotinib, an EGFR antagonist, significantly decreased both HSC regeneration and mice survival following TBI. *VavCre;EGFR*$^{fl/+}$ mice also demonstrated delayed recovery of BM stem/progenitor cells following TBI compared to *VavCre;EGFR*$^{+/+}$ mice. Mechanistically, EGF reduced radiation-induced apoptosis of HSCs and mediated this effect via repression of the proapoptotic protein, PUMA. EGFR signaling regulates HSC regeneration following myelosuppressive injury.

HSCs can be found in proximity to BM sinusoidal vessels[1] and BM endothelial cells (ECs) regulate both HSC homeostasis and regeneration[2-8]. Ding et al. reported that maintenance of the HSC pool in mice was dependent upon the expression of stem cell factor (SCF) by BM

Corresponding author: John P. Chute M.D., Professor of Medicine, Pharmacology and Cancer Biology, Division of Hematologic Malignancies and Cellular Therapy, Department of Medicine, Duke University, Durham, NC 27710, john.chute@duke.edu, Phone: 919-668-4706, Fax: 919-668-1091.

AUTHOR CONTRIBUTIONS

P.L.D. performed experiments, analyzed data, and wrote the paper; H.A.H., K.H., and J.L.R performed experiments and analyzed data; E.F., M.Q., J.R.H., D.D. performed experiments; J.M.S. provided reagents; N.J.C. analyzed data and wrote the paper; D.G.K. designed experiments, analyzed data and wrote the paper; J.P.C. conceived of the study, designed experiments, analyzed the data, and wrote the paper.

Conflict of interest disclosure: The authors declare no competing financial interests.

ECs or perivascular cells, demonstrating the important role of ECs and perivascular cells in maintaining the HSC pool during homeostasis[8]. We have shown that adult sources of ECs produce soluble growth factors which promote the expansion of human HSCs in vitro[2] and support the regeneration of murine and human HSCs in vitro following radiation exposure[2,3,9-11]. We have also demonstrated that systemic infusion of autologous or allogeneic ECs accelerates BM HSC reconstitution and hematologic recovery in mice following radiation-induced myelosuppression[4,12]. Hooper et al. demonstrated a requirement for VEGFR2$^+$ sinusoidal ECs for normal hematologic recovery to occur following total body irradiation[6]. Similarly, systemic delivery of anti-VEcadherin antibody, which inhibits BM vasculogenesis, significantly delays hematologic recovery following myelosuppression[4,5]. However, the precise mechanisms through which BM ECs regulate hematopoietic regeneration remain unknown. Here, utilizing a screen for cytokines in the BM serum from *Tie2Cre;Bak1*$^{-/-}$*;Bax*$^{fl/-}$ mice, which lack BAK and BAX in Tie2$^+$ ECs[13] and demonstrate a strong radioprotective phenotype, we identified epidermal growth factor (EGF) as a candidate EC-derived mediator of radioprotection of the hematopoietic system. We now show that systemic administration of EGF accelerates the recovery of long term-HSCs and improves the survival of mice following radiation-induced myelosuppression, whereas pharmacologic inhibition or genetic deletion of EGFR antagonizes hematopoietic regeneration in vivo. This study demonstrates a previously unrecognized role for EGFR signaling in regulating hematopoietic regeneration in vivo.

RESULTS

Tie2Cre;Bak1$^{-/-}$*;Bax*$^{fl/-}$ mice secrete EGF and EGF mediates HSC regeneration in vitro

We developed a genetic model to delete BAK and BAX, which regulate the intrinsic pathway of apoptosis[13], in Tie2$^+$ ECs as a means to protect BM ECs from radiation-induced injury. Following high dose TBI, *Tie2Cre;Bak1*$^{-/-}$*;Bax*$^{fl/-}$ mice demonstrated significant protection of the BM vascular and HSC compartments as well as marked improvement in survival compared to *Tie2Cre;Bak1*$^{-/-}$*;Bax*$^{fl/+}$ mice, which retained 1 allele of *Bax*, and wild type mice[14]. In order to identify secreted factors elaborated by Tie2$^+$ BM ECs that might have contributed to the radioprotection in *Tie2Cre;Bak1*$^{-/-}$*;Bax*$^{fl/-}$ mice, we generated primary BM EC lines (CD45$^-$ VWF$^+$ Lectin$^+$ AcLDL$^+$) from *Tie2Cre;Bak1*$^{-/-}$*;Bax*$^{fl/-}$ mice (FL/− ECs) and *Tie2Cre;Bak1*$^{-/-}$*;Bax*$^{fl/+}$ mice (FL/+ ECs), as previously described [2,3,9,15]. When wild type BM ckit$^+$sca-1$^+$lin$^-$ (KSL) progenitor cells, were irradiated with 300 cGy in vitro and then plated in non-contact culture with FL/− ECs, we observed significant increases in recovery of total cells, CFCs and CFU-S12 at day +7 compared to non-contact FL/+ EC cultures (Fig. 1a). These results suggested that BM ECs from *Tie2Cre;Bak1*$^{-/-}$*;Bax*$^{fl/-}$ mice produced soluble factors that promoted hematopoietic stem/progenitor cell regeneration following radiation injury. In a complementary study, the addition of BM serum from irradiated *Tie2Cre;Bak1*$^{-/-}$*;Bax*$^{fl/-}$ mice to cultures of irradiated BM KSL cells promoted the recovery of total cells and CFCs in 7 day culture, whereas BM serum from *Tie2Cre;Bak1*$^{-/-}$*;Bax*$^{fl/+}$ mice had no beneficial effect (Supplemental Fig. 1a).

In order to identify paracrine factors in the BM of *Tie2Cre;Bak1*$^{-/-}$*;Bax*$^{fl/-}$ mice which may have contributed to the radioprotection of hematopoietic stem/progenitor cells in vivo, we performed a cytokine array on the BM serum from *Tie2Cre;Bak1*$^{-/-}$*;Bax*$^{fl/-}$ mice, *Tie2Cre;Bak1*$^{-/-}$*;Bax*$^{fl/+}$ mice and wild type C57Bl6 mice prior to and following 750 cGy TBI. Within the list of cytokines that were significantly enriched in BM serum from *Tie2Cre;Bak1*$^{-/-}$*;Bax*$^{fl/-}$ mice versus *Tie2Cre;Bak1*$^{-/-}$*;Bax*$^{fl/+}$ mice[14], we identified epidermal growth factor (EGF) to be approximately 18-fold increased in concentration in the BM of irradiated *Tie2Cre;Bak1*$^{-/-}$*;Bax*$^{fl/-}$ mice compared to irradiated *Tie2Cre;Bak1*$^{-/-}$*;Bax*$^{fl/+}$ mice and was expressed at 3-fold higher levels by *Bak1*$^{-/-}$*;Bax*$^{fl/-}$ ECs compared to *Bak1*$^{-/-}$*;Bax*$^{fl/+}$ ECs (Fig. 1b). Furthermore, EGF was not detected in ELISA of supernatants of BM KSL cells from *Tie2Cre;Bak1*$^{-/-}$*;Bax*$^{fl/-}$ mice (data not shown), suggesting that EGF was not produced in an autocrine manner by BM stem/progenitor cells. Interestingly, *Tie2Cre;Bak1*$^{-/-}$*;Bax*$^{fl/-}$ mice displayed increased density of mouse endothelial cell antigen – positive (MECA^{+}) vessels in the BM compared to *Tie2Cre;Bak1*$^{-/-}$*;Bax*$^{fl/+}$ mice and C57Bl6 mice (Supplemental Fig. 1b). Therefore, the increased concentrations of EGF in the BM serum of *Tie2Cre;Bak1*$^{-/-}$*;Bax*$^{fl/-}$ mice compared to controls may have been caused, in part, by increased density of EGF-secreting BM ECs in *Tie2Cre;Bak1*$^{-/-}$*;Bax*$^{fl/-}$ mice.

In order to determine whether EGFR was expressed by wild type BM HSCs and progenitor cells, FACS analysis was performed. Less than 2% of BM lin^{+} and lin^{-} cells expressed EGFR, but 7.9% of BM KSL cells and 9.2% of BM SLAM^{+}KSL cells, which are enriched for long-term HSCs[1], expressed EGFR (Fig. 1c). EGFR surface expression increased 4-fold and 6-fold on BM KSL and SLAM^{+}KSL cells, respectively, at 4 hours following 300 cGy irradiation, demonstrating induction of EGFR expression on HSCs following irradiation (Fig. 1c,d). Following EGF treatment, EGFR phosphorylation was demonstrated in BM KSL cells and BM SLAM^{+}KSL cells in vitro and also on BM KSL cells in vivo, demonstrating that EGFR was functional on BM hematopoietic stem/progenitor cells (Fig. 1e).

We next performed gain-of-function studies to determine whether treatment of irradiated BM KSL cells with EGF could support BM stem/progenitor cell regeneration in vitro. When 20 ng/mL EGF was added to irradiated (300 cGy) BM KSL cells cultured with cytokines (Thrombopoietin, Stem cell factor, Flt-3 ligand, TSF), we observed significant increases in the recovery of CFCs and CFU-S12 compared to cultures with cytokines alone (Fig. 1f). Of note, the addition of EGF to non-contact fl/+ EC cultures of irradiated BM KSL cells also increased CFC and CFUS-12 recovery compared to culture with fl/+ ECs alone, whereas the addition of anti-EGF antibody to fl/− EC cultures caused a significant decrease in the recovery of CFC and CFU-S12 recovery compared to fl/− EC cultures alone (Supplemental Fig. 2). These data suggested that fl/− EC – mediated regeneration of irradiated BM progenitor cells was dependent on EGF. Utilizing competitive repopulation assays, we also found that mice transplanted with the progeny of irradiated/EGF-treated BM 34^{-}KSL cells demonstrated 3- and 5-fold higher donor hematopoietic cell engraftment at 8 and 12 weeks post-transplant compared to mice transplanted with the progeny of cytokine cultures alone (Fig. 1g).

Treatment of non-irradiated BM KSL cells with EGF in vitro also caused a significant expansion of BM KSL cells and CFU-S12 compared to the progeny of cytokine cultures alone (Fig. 1h). Mice competitively transplanted with the progeny of BM 34^{-}KSL cells cultured with cytokines plus EGF displayed more than 10-fold increased donor hematopoietic cell repopulation at 12 weeks post-transplant compared to mice transplanted with the progeny of BM 34^{-}KSL cells cultured with cytokines alone (Fig. 1h). These results suggest that EGF also promotes the maintenance of non-irradiated HSCs in culture.

Systemic administration of EGF induces HSC regeneration in vivo

In order to determine if EGF treatment could promote HSC regeneration in vivo, we measured hematopoietic reconstitution in C57Bl6 mice following 700 cGy TBI and subsequent treatment with EGF or saline, intraperitoneally, at +2 hours and then daily for 7 days (Fig. 2a). At day +7 following TBI, EGF-treated animals demonstrated increased BM cellularity compared to controls (Fig. 2b) as well as significantly increased BM cells, BM KSL cells, CFCs and CFU-S12 compared to saline-treated mice (Fig. 2b-d).

In order to determine if treatment with EGF could rescue the functional BM HSC pool in irradiated mice, we competitively transplanted lethally irradiated ($CD45.1^{+}$) recipient mice with BM cells from either non-irradiated donor mice, 700 cGy-irradiated/EGF-treated donor mice or 700 cGy-irradiated/saline-treated mice ($CD45.2^{+}$). At 12 weeks post-transplant, mice transplanted with 5×10^5 BM cells from non-irradiated donors demonstrated high level donor cell engraftment in the BM (mean 74.9%, Fig. 2e). Conversely, mice transplanted with the same dose of BM cells from irradiated/saline-treated donors demonstrated much lower donor cell engraftment (mean 0.4%). Interestingly, mice transplanted with the identical dose of BM cells from irradiated/EGF-treated mice displayed significantly increased donor cell engraftment (mean 8.5%) compared to mice transplanted with BM from irradiated/saline-treated donors (Fig 2e). Of note, this difference in total engraftment was primarily a function of increased donor myeloid cell recovery in the EGF-treatment group, suggesting that EGF treatment may have specifically augmented the recovery of short-term HSCs with myeloid reconstituting potential (Fig. 2e). We also found a close correspondence between total donor cell engraftment and the donor cell chimerism within BM KSL cells in each group of mice (Fig. 2e,f)[16]. Donor cell engraftment within BM KSL cells in recipients of BM cells from irradiated/EGF-treated mice was 6-fold higher than that observed in recipients of BM cells from irradiated/saline-treated mice, but remained 9-fold lower than in mice transplanted with non-irradiated BM cells. Therefore, while EGF treatment significantly increased the recovery of BM HSCs after TBI, it did not fully restore HSC function compared to non-irradiated donor mice.

We also performed competitive secondary transplants in which BM cells from primary recipient mice were transplanted into lethally irradiated syngeneic mice (Fig. 2g). At 12 weeks, secondary recipient mice in the non-irradiated donor group displayed a high donor cell engraftment (mean 53.4%, Fig. 2g). Conversely, mice in the irradiated donor/saline-treatment group had very low donor cell engraftment (mean 0.5%). Secondary recipients within the irradiated donor/EGF-treatment group demonstrated significantly higher total and multilineage donor engraftment (mean 24%, Fig. 2g) compared to the irradiated/saline-

treatment group. Secondary mice within the irradiated/EGF-treatment group displayed a corresponding increase in donor cell chimerism within BM KSL cells compared to the irradiated/saline-treatment group (Fig. 2h). These results suggest that EGF treatment promoted the recovery of LT-HSCs in mice following TBI.

EGFR inhibition impairs HSC regeneration in vivo

In order to determine if EGFR inhibition could suppress HSC regeneration in vivo, we irradiated mice with 700 cGy and then treated with erlotinib, an EGFR antagonist, or water, via oral gavage from day 0 to day +14 (Fig. 3a). At day +7, both erlotinib-treated and control mice demonstrated depletion of BM stem/progenitor cells (data not shown). At day +14, irradiated, control mice demonstrated recovery of BM cellularity, CFCs and CFUS-12, whereas erlotinib-treated mice displayed depletion of BM CFCs and CFU-S12 (Fig. 3b,c). Importantly, erlotinib-treated mice also displayed a deficit in short-term and longer-term HSCs post-TBI as compared to irradiated, control mice, as measured by competitive repopulation assay (Fig. 3d). These results suggested that EGFR inhibition impaired hematopoietic stem/progenitor cell regeneration following TBI.

In order to determine whether EGFR signaling was involved in mediating the radioprotection we had observed in *Tie2Cre;Bak1*$^{-/-}$*;Bax*$^{fl/-}$ mice[14], we administered erlotinib or water to *Tie2Cre;Bak1*$^{-/-}$*;Bax*$^{fl/-}$ mice beginning 3 days prior to 300 cGy TBI and evaluated BM HSC and progenitor cell content at +2 hours following TBI (Fig 3e). Erlotinib-treated *Tie2Cre;Bak1*$^{-/-}$*;Bax*$^{fl/-}$ mice contained significantly decreased BM KSL cells and CFU-S12 following TBI compared to control, irradiated *Tie2Cre;Bak1*$^{-/-}$*;Bax*$^{fl/-}$ mice (Fig. 3f). This corresponded with a decrease in EGFR-phosphorylation in BM KSL cells in erlotinib-treated *Tie2Cre;Bak1*$^{-/-}$*;Bax*$^{fl/-}$ mice (Fig. 3g). As expected, irradiated *Tie2Cre;Bak1*$^{-/-}$*;Bax*$^{fl/-}$ mice demonstrated relative protection of BM HSCs with multilineage repopulating capacity following TBI (Fig. 3h). Conversely, erlotinib-treated, irradiated *Tie2Cre;Bak1*$^{-/-}$*;Bax*$^{fl/-}$ mice displayed a marked deficit in BM HSCs capable of multilineage reconstitution in vivo (Fig. 3h). These results suggested that EGFR signaling was important for the radioprotection of BM stem/progenitor cells in *Tie2Cre;Bak1*$^{-/-}$*;Bax*$^{fl/-}$ mice.

EGFR deficiency inhibits hematopoietic progenitor cell regeneration following irradiation

Erlotinib has been shown to inhibit kinases other than EGFR, including Jak2 and Src kinases[17,18]. In order to determine whether erlotinib effects on HSCs were specific to EGFR or via off-target effects, we generated *VavCre;EGFR*$^{fl/fl}$ mice (*EGFR*$^{fl/fl}$) and *VavCre;EGFR*$^{+/+}$ (*EGFR*$^{+/+}$) mice and verified the deletion of EGFR expression in BM lineage negative (lin$^-$) cells (Fig. 4a). We cultured BM lin$^-$ cells from *EGFR*$^{fl/fl}$ or *EGFR*$^{+/+}$ mice in cytokine media for 72 hours and observed decreased total cell growth and CFC production in EGFR-deficient cells (Figure 4b). Treatment of *EGFR*$^{fl/fl}$ BM lin$^-$ cells with erlotinib caused no significant effect on total cell expansion or CFC production compared to control cultures (Figure 4c). Conversely, erlotinib treatment of *EGFR*$^{+/+}$ BM lin$^-$ cells decreased total cell expansion and CFC production compared to *EGFR*$^{+/+}$ BM lin$^-$ cells cultured with cytokines alone and *EGFR*$^{fl/fl}$ BM lin$^-$ cells cultured with erlotinib. These data suggest that erlotinib acted specifically upon EGFR in BM progenitor cells.

We also compared the in vivo recovery of BM hematopoietic stem/progenitor cells in *VavCre;EGFR*$^{+/+}$ mice and *VavCre;EGFR*$^{fl/+}$ mice (*EGFR*$^{fl/+}$) following 500 cGy TBI. At baseline, *EGFR*$^{fl/+}$ mice demonstrated decreased EGFR expression in BM lin^{-} cells relative to *EGFR*$^{+/+}$ mice (Fig. 4d) and displayed no differences in complete blood counts or BM CFCs compared to *EGFR*$^{+/+}$ mice (Fig. 4e,f). However, at day +7 following TBI, *EGFR*$^{fl/+}$ mice contained 5-fold decreased BM CFC content and 30-fold decreased BM SLAM^{+}KSL cells, compared to *EGFR*$^{+/+}$ mice (Fig. 4g). These data suggest that EGFR may be necessary for normal BM stem/progenitor cell regeneration to occur following TBI.

EGF induces HSC cycling following irradiation

Activation of EGFR can promote both cell proliferation and survival following injury[19,20], so we tested whether EGF treatment modulated HSC cycle status following irradiation. BM KSL cells were irradiated with 300 cGy and then treated in vitro with cytokines alone or cytokines plus EGF. At baseline, more than 90% of BM KSL cells resided in G_0/G_1 (Fig. 5a). At 72 hours after irradiation, EGF treatment of irradiated BM KSL cells caused a significant increase in cells in G_2/S/M phase and a corresponding decrease in G_0 cells compared to cytokine treatment alone (Fig. 5a). EGF treatment had comparable proliferative effects on irradiated BM KSL cells from *Tie2Cre;Bak1*$^{-/-}$*;Bax*$^{fl/-}$ mice (Supplemental Fig. 3a). Importantly, EGF treatment of mice for 7 days following 700 cGy TBI also significantly increased BrdU incorporation in BM KSL cells compared to saline-treated, irradiated mice (Fig. 5b).

EGFR can mediate cell proliferation via activation of the MAPK and PI3k/Akt pathways [21,22]. In irradiated BM KSL cells, EGF treatment did not alter MAPK phosphorylation (data not shown) but did increase Akt phosphorylation (Figure 5c). This induction of Akt in response to EGF treatment corresponded with increased CFC recovery in EGF-treated BM KSL cells following irradiation (Fig. 5c). Treatment of irradiated BM KSL cells with Ly294002, a PI3K inhibitor, blocked EGF-mediated Akt phosphorylation and inhibited BM progenitor cell recovery in response to EGF (Fig. 5c). Irradiated BM KSL cells that were treated with EGF + Ly294002 also demonstrated significantly decreased cell cycling compared to KSL cells treated with EGF alone (Fig. 5c). These data suggest that EGF-driven effects on HSC cycling and progenitor cell recovery are mediated, at least in part, via activation of the PI3k/Akt pathway.

EGF inhibits radiation-induced HSC apoptosis via repression of PUMA

We performed Annexin/7AAD staining to assess the effects of EGF on HSC survival after irradiation. At 72 hours following 300 cGy, EGF-treated cultures contained 2-fold decreased Annexin^{+} KSL cells compared to cytokine cultures (Fig. 5d). C57Bl6 mice that were irradiated with 700 cGy and then treated with EGF x 7 days also contained 4-fold decreased Annexin^{+} BM hematopoietic cells compared to saline-treated controls (Fig. 5d). Of note, EGF treatment also decreased the frequency of Annexin^{+} cells in cultures of irradiated BM KSL cells from *Tie2Cre;Bak1*$^{-/-}$*;Bax*$^{fl/-}$ mice (Supplemental Fig. 3b). The latter result suggests that EGF may mediate HSC survival following irradiation via additional mechanisms, such as DNA repair, which are not directly related to inhibition of apoptosis[23].

The p53-upregulated modulator of apoptosis (PUMA) is an essential mediator of radiation-induced hematopoietic toxicity [24,25]. Since EGF promoted HSC survival following irradiation, we examined whether EGF caused such effects via inhibition of PUMA. PUMA expression increased significantly in BM HSCs from $p53^{+/+}$ mice after 300 cGy, whereas PUMA expression did not change in irradiated HSCs from $p53^{-/-}$ mice, indicating that PUMA induction in HSCs was p53-dependent (Fig. 5e). EGF treatment repressed radiation-induced PUMA expression in BM KSL cells from $p53^{+/+}$ mice but had no effect on PUMA expression in BM KSL cells from $p53^{-/-}$ mice (Fig. 5e). PUMA protein levels in BM KSL cells correspondingly increased in response to radiation in a p53-dependent manner and EGF treatment also significantly decreased PUMA protein levels in KSL cells following irradiation (Fig. 5e).

As expected, BM KSL cells from $PUMA^{-/-}$ mice contained a lower percentage of apoptotic cells and increased CFC content at 72 hours following 300 cGy compared to $PUMA^{+/+}$ BM KSL cells (Fig. 5f-h). EGF treatment increased HSC survival and CFC regeneration in $PUMA^{+/+}$ KSL cell cultures following irradiation, but had no effect on HSC survival or CFC production in $PUMA^{-/-}$ KSL cell cultures following irradiation (Fig. 5f-h). These results suggested that EGF-mediated inhibition of radiation-induced HSC apoptosis was dependent upon inhibition of PUMA.

Systemic administration of EGF improves the survival of lethally irradiated mice

To test whether EGFR signaling affected mice survival following TBI, C57Bl6 mice were treated with 10 μg/g erlotinib or water from day −3 to day +14 following 700 cGy TBI. Fifty-three percent of control, irradiated mice remained alive through day +30. In contrast, none of the erlotinib-treated mice survived beyond day +27 (Figure 6). An additional group of C57Bl6 mice was irradiated with 700 cGy and treated with either 0.5 μg/g EGF or saline intravenously x 7 days, beginning 2 hours post-TBI. Fifty-seven percent of saline-treated mice survived through day +30 (Figure 6). Conversely, 93% of EGF-treated mice remained alive through day +30. These results suggested that pharmacologic modulation of EGFR signaling altered survival following TBI.

DISCUSSION

Recent studies have suggested that hematopoietic regeneration in vivo is regulated by BM ECs[4-6]. However, the mechanisms through which BM ECs regulate hematopoietic regeneration remain largely unknown. Identification of the mechanisms which govern hematopoietic regeneration could have broad implications for the treatment of patients receiving myelosuppressive chemo- or radiotherapy or undergoing stem cell transplantation[26]. Here, we demonstrate that EGF, which we identified via a screen of BM serum from radioprotected mice bearing deletion of *BAK* and *BAX* in $Tie2^{+}$ ECs, mitigates radiation injury to HSCs and systemic administration of EGF can improve the survival of irradiated mice. Of note, since EGF is a mitogen for non-hematopoetic cells that are affected by radiation injury (e.g. intestinal epithelium), EGF-mediated improvement in mice survival could have been contributed to by such effects. Nonetheless, our results suggest that systemic administration of EGF could have therapeutic potential to accelerate hematopoietic

recovery in patients who have received TBI as well as for the victims of acute radiation sickness [27,28]. In that regard, it is worth noting that EGF treatment caused a significant enhancement in myeloid reconstitution in primary transplanted mice, suggesting a specific effect on ST-HSCs with myeloid repopulating potential. Furthermore, while EGF treatment was associated with improved multilineage hematopoietic reconstitution in secondary mice, stronger myeloid recovery was observed and T cell reconstitution was relatively low. This skewing toward myeloid recovery at the expense of T lymphoid recovery in recipients of BM cells from irradiated donors mimics some aspects of the HSC aging phenotype and may reflect TBI-mediated DNA damage to the HSC pool[29,30].

Since erlotinib has recently been shown to mediate cellular effects via inhibition of enzymes other than EGFR [17,18], we utilized a genetic model of *VavCre;EGFR*$^{fl/fl}$ mice to determine the specific role of EGFR in regulating the hematopoietic response to radiation. In vitro studies demonstrated that erlotinib treatment had no effect on EGFR-deficient hematopoietic cells in culture, whereas erlotinib treatment of EGFR$^{+/+}$ hematopoietic cells significantly inhibited both cell expansion and CFC production in culture. Therefore, erlotinib acted specifically through EGFR inhibition to diminish hematopoietic progenitor cell recovery in our model. Importantly, *VavCre;EGFR*$^{fl/+}$ mice, which are heterozygous for EGFR expression, displayed significantly decreased BM HSC and progenitor cell recovery early after TBI compared to *VavCre;EGFR*$^{+/+}$ mice, which retained both EGFR alleles. These results suggest that EGFR signaling has an important role in regulating hematopoietic regeneration following radiation injury.

Gamma radiation causes direct and indirect DNA damage which can result in cell cycle arrest or apoptosis of hematopoietic progenitor cells[31]. In the presence of radiation-induced DNA damage, cell-cycle arrest can occur via p53-dependent or -independent mechanisms[32,33]. Importantly, cell cycle arrest of hematopoietic cells can be overridden by treatment with cytokines[34] and cytokine-mediated induction of hematopoietic progenitor cell proliferation early after radiation exposure may have beneficial effects toward promoting short-term hematopoietic recovery and improved near-term survival[10,35,36]. While the mechanism behind these effects is not clear, cytokine treatment may induce synchronous entry of hematopoietic stem/progenitor cells into late S phase, a more radioresistant phase of cell cycle[36,37]. Cytokine-driven differentiation of HSCs into myelo-erythroid progenitor cells (MEPs) also could provide short-term benefit since systemic infusion of MEPs alone can completely radioprotect mice following lethal dose TBI[38]. In non-hematopoietic tissues, EGFR signaling can regulate cell proliferation in a context-dependent manner, producing both cell cycle arrest and augmented proliferation[22,39]. Here, we show that EGF treatment induces early HSC cycling following radiation exposure and this effect was mediated via activation of the PI3k/Akt pathway. While EGF can certainly modulate radiation response via additional mechanisms such as induction of DNA repair mechanisms[23], our data suggest that EGF-mediated induction of HSC proliferation contributes to the early recovery of the hematopoietic progenitor pool after irradiation.

Deletion of PUMA has been shown to protect BM hematopoietic stem/progenitor cells from radiation-induced death and confer a survival advantage in mice following TBI[24,25]. Here, we have shown that EGF treatment represses radiation-induced expression of PUMA in

HSCs. Furthermore, we show that EGF effects are largely dependent upon repression of PUMA. This result is consistent with previous studies that have shown that cytokines such as IL-3 can inhibit PUMA expression in hematopoietic cells and that cytokine withdrawal mediates hematopoietic cell death in a PUMA-dependent manner[40,41]. Of note, Akt, which is induced by EGF treatment of HSCs, was reported to suppress p53-dependent induction of PUMA and promote PUMA protein destabilization in leukemia cells[42]. Importantly, while our results suggest that EGF-mediated inhibition of HSC apoptosis is dependent upon repression of PUMA, it remains possible that changes in expression of other cell cycle regulators (e.g. induction of p21) in PUMA$^{-/-}$ mice may have contributed to the inhibition of EGF effects in this model[43].

Here we have elucidated a previously unknown function of EGF in promoting HSC regeneration following radiation-induced myelosuppression. EGF is an established mitogen and pro-survival factor for epithelial cells and endothelial cells and mutations in EGFR can be tumorigenic [44-48]. EGF also regulates stem cell functions in non-hematopoietic tissues such as the brain and liver[49-51]. Prior studies have suggested that EGFR was not expressed on hematopoietic stem cells[52-54], although these studies lacked the benefit of multiparametric flow cytometry to isolate BM HSCs as performed here. While EGFR was recently shown to be expressed on BM ckit^{+}lin^{-} progenitor cells[55,56], EGF is not known to regulate HSC self-renewal or regeneration. In a prior study, the addition of EGF to stromal cell co-cultures inhibited hematopoietic progenitor cell growth in vitro, although these effects were mediated via indirect effects on stromal cells[57]. Recently, Ryan et al. reported that EGFR inhibition facilitated GCSF-mediated mobilization of hematopoietic progenitor cells in mice[55], although no effects were demonstrated in the absence of GCSF and no effects on HSC content, proliferation or function were described[55]. Here we show that BM HSCs express functional EGFR and that EGF acts directly on HSCs to increase HSC cycling and survival following irradiation. These observed effects of EGF on HSC growth are comparable to those described for fibroblast growth factor 1 (FGF1), which also activates PI3k/Akt signaling, suggesting a possible convergence of action of EGF and FGF1 on critical signaling pathways in HSCs[58,59]. Translationally, these results suggest that EGF may have therapeutic potential in hematopoietic cell transplant patients who receive TBI-based conditioning prior to transplant. In light of the report by Shen et al. of a deleterious bystander effect of TBI-induced reactive oxygen species on transplanted donor HSCs, it will be interesting to determine whether EGF administration can ameliorate such effects to augment hematopoietic reconstitution[60]. EGF also has potential utility for the treatment of acute radiation sickness, which can cause life threatening BM failure and for which few treatments exist.

METHODS

Animals

Ten to 12 week-old C57Bl6 (CD45.2^{+}) mice and B6.SJL (CD45.1^{+}) mice were obtained from Jackson Laboratory (Bar Harbor, ME). *Tie2Cre;Bak1*$^{-/-}$*;Bax*$^{fl/-}$ and *Tie2Cre;Bak1*$^{-/-}$*;Bax*$^{fl/+}$ were generated as previously described[13]. *EGFR*$^{fl/fl}$ mice[61] (Mutant Mouse Regional Resource Centers, Chapel Hill, NC) were bred with *VavCre* mice

(Jackson Laboratory) to generate *VavCre;EGFR*$^{fl/-}$ mice. In *VavCre* mice, floxed alleles are excised by Cre in Vav^{+} cells and their progeny[62,63]. To generate *VavCre;EGFR*$^{fl/fl}$ mice, we mated *VavCre;EGFR*$^{fl/+}$ with *EGFR*$^{fl/fl}$ mice. Mice were genotyped for the Cre allele through Transnetyx, Inc. (Cordova, TN) and loxP-EGFR alleles as previously described[61]. The deletion of EGFR in BM cells was quantified using RT-PCR (Applied Biosystems, Carlsbad,CA). *p53*$^{+/-}$ and *p53*$^{-/-}$ mice[41] were purchased from Jackson Laboratories and genotyped through Transnetyx Incorporated. *PUMA*$^{+/+}$ and *PUMA*$^{-/-}$ mice were purchased from Jackson Laboratory. Deletions of p53 and PUMA were quantified with RT-PCR (Applied Biosystems, Carlsbad,CA). All animal studies described herein were approved by the Duke University Animal Care and Use Committee.

Hematopoietic progenitor cell assays

BM cells were collected into PBS (Cellgro, Manassas, VA) with 10% fetal bovine serum (Hyclone, Logan, UT) and 1% penicillin/streptomycin (GIBCO, Grand Island, NY). Viable BM cells were quantified using Trypan Blue Stain (Lonza, Basel, Switzerland) to exclude apoptotic and dead cells. Cells were then incubated with anti-c-kit, anti-Sca-1, anti-lineage cocktail, anti-CD41, anti-CD48, and anti-CD150 antibodies (Biolegend and eBiosciences, San Diego, CA; BD, San Jose, CA) to measure ckit^{+}sca-1^{+}lin^{-} (KSL) progenitor cells or CD150^{+}CD41^{-}CD48^{-}KSL (SLAM/KSL) as previously described[1]. Colony forming cells (CFCs) and CFU-S12 assays were also performed to measure functional hematopoietic stem/progenitor cell content. For CFCs, either whole BM or cultured lineage-cells, or KSL cells were plated onto methylcellulose (StemCell Technologies, Vancouver, BC, Canada), and colonies were scored on day 14. 1×10^5 BM or 2×10^5 cells were collected from donor mice and injected via tail vein into recipient C57Bl6 mice that had been given 950 cGy TBI. At day +12 post-injection, spleens from recipient mice were harvested and stained with Bouin's fixative solution (Ricca Chemical Company, Arlington, TX), and colonies were counted as previously described[64]. Complete blood counts were performed on a HemaVet 950 (Drew Scientific, Dallas, TX).

Generation and culture of primary BM ECs from *Tie2Cre;Bak1*$^{-/-}$*;Bax*$^{fl/-}$ mice

For isolation and generation of primary BM ECs from FL/− and FL/+ mice, whole BM was collected from bilateral femurs and passed through a 70 micron filter. BM vessel fragments were then plated, rinsed with 10% FBS, washed in PBS and treated with 0.25% trypsin-EDTA. BM vessel explants were cultured on 10% gelatin-coated wells (Sigma-Aldrich) with EGM-2 Endothelial cell growth medium-2 (Lonza) as previously described[2,3,9,10,15]. Wells were washed daily for 7-10 days and primary cells were passaged when confluent.

BM KSL cells from adult C57Bl6 mice were exposed to 300 cGy in vitro and then cultured with TSF (20 ng/ml thrombopoietin, 125 ng/ml stem cell factor, and 50 ng/ml Flt-3 ligand (TSF, R&D Systems, Minneapolis, MN) alone or in non-contact culture with fl/− ECs or fl/+ ECs. In some experiments, cultures were supplemented with 20 ng/ml EGF or 1 μg/ml of a blocking anti-EGF (R&D Systems, Minneapolis, MN). After 7 days in culture, cell progeny were collected and colony-forming cell assays (CFC) and CFU-S12 assays were performed as previously described[2].

Cytokine array and EGF/EGFR expression analysis

Whole BM was collected from adult, non-irradiated *Tie2Cre;Bak1*$^{-/-}$*;Bax*$^{fl/-}$ mice and *Tie2Cre;Bak1*$^{-/-}$*;Bax*$^{fl/+}$ mice and C57Bl6 mice and at 6 hours and 7 days following 750 cGy TBI. After centrifugation, BM supernatants were collected into IMDM and analyzed for cytokine concentrations using Quantibody mouse cytokine array 1000, according to manufacturer's guidelines (RayBiotech, Inc., Norcross, GA). For analysis of protein expression of EGFR by C57Bl6 BM lin$^+$ cells, lin$^-$ cells, KSL cells, and SLAM$^+$KSL cells, BM lin$^-$ cells were isolated using MACS microbeads and LS columns according to manufacturer specifications (Miltenyi Biotec, Auburn, CA). BM lin$^-$ cells were stained with anti-EGFR FITC (Abcam, Cambridge, MA) and antibodies for SLAM and KSL markers as noted above. For analysis of EGFR expression after radiation, C57Bl6 mice were exposed to 300 cGy or 700 cGy TBI and then sacrificed at 4 hours. BM lin$^-$ cells were isolated and stained with 7AAD and antibodies for SLAM and KSL markers as noted above. For analysis of phosphorylation of the Tyr-1173 residue of EGFR, BM lin$^+$ and lin$^-$ cells were isolated using Macs Lineage depletion columns as described above. BM KSL and SLAM$^+$KSL cells were isolated using fluorescence activated cell sorting. Cells were cultured for 45 minutes in X-Vivo media (Lonza) alone or in media supplemented with 20 ng/mL EGF, then fixed in 4% paraformaldehyde and permeabilized in 0.25% saponin. Cells were stained with anti-phospho-Tyr-1173 rabbit anti-mouse polyclonal antibody or isotype control and then incubated with a secondary goat anti-rabbit Alexafluor 488 antibody (Life Technologies, Grand Island, NY). For analysis of phosphorylation of EGFR in vivo, mice were injected with 20 ug of EGF or saline via tail vein injection and then sacrificed 10 minutes after injection. BM cells were stained for KSL, fixed, permeabilized, and stained for phospho-EGFR as noted above.

HSC cycling and survival assays

Cell cycle analysis was performed by flow cytometric analysis modified from previous reports[65-67]. Briefly, cells were fixed and permeabilized with 0.25% Saponin (Calbiochem, La Jolla, CA), 2.5% paraformaldehyde, 2% FBS in 1XPBS, and then labeled with Ki67-FITC and 7-AAD (BD). Cell proliferation was measured in C57Bl6 mice exposed to 700 cGy TBI and administered 5-bromo-2-deoxyridine (BrdU, BD) in drinking water from the day of irradiation until day +7. BM cells were labeled with anti-cKit PE, anti-sca1 PE-Cy7, anti-lineage APC, and anti-BrdU FITC. Incorporation of BrdU was analyzed by flow cytometry according to the manufacturer's staining protocol (BD).

Since 300 cGy irradiation in vitro induces apoptosis in BM hematopoietic progenitor cells, we irradiated 3×10^3 C57Bl6 KSL cells with 300 cGy, and then placed in culture with TSF alone, TSF with 20 ng/ml EGF, or TSF, EGF, and 1uM Ly294002 (Cell Signaling Technology, Danvers, MA) for 72 hours. Cell apoptosis and necrosis were analyzed by flow cytometry according to manufacturer's protocols with Annexin V-FITC and 7-AAD staining (BD, San Jose, CA). For analysis of phosphorylation AKT-S473, BM KSL cells were cultured for 15 minutes with TSF or TSF + 20 ng/mL EGF or with 20 μM Ly294002. Cells were fixed and permeabilized with Fix Buffer I and Perm Buffer III (BD), and then stained with mouse anti-phospho-AKT-S473 PE (BD) or isotype control.

P53 and PUMA gene expression analyses were performed on BM KSL cells from C57Bl6 mice, $p53^{+/+}$ mice and $p53^{-/-}$ mice following exposure to 300 cGy and culture with TSF or TSF + 20 ng/ml EGF for 6 hours, along with non-irradiated controls. Analysis of PUMA protein levels by flow cytometry was performed 12 hours after 300 cGy on Bl6 KSL in culture with TSF or TSF+ 20 ng/ml EGF, along with non-irradiated controls. Cells were fixed in 4% paraformaldehyde and permeabilized in 0.25% saponin. Cells were stained with a primary anti-PUMA antibody (Abcam) followed by a secondary goat anti-rabbit Alexafluor 488 antibody (Life Technologies). Functional studies were also performed using BM KSL cells from $PUMA^{+/+}$ mice and $PUMA^{-/-}$ mice to quantify % $Annexin^{+}$ cells and CFC recovery in vitro following 300 cGy irradiation. BM lin^{-} cells from *VavCre;*$EGFR^{+/+}$ or *VavCre;*$EGFR^{fl/fl}$ mice were cultured with TSF or TSF + 10 μM erlotinib, or TSF following 300 cGy for 72 hours, and then collected for total cell counts and CFCs analysis.

Competitive repopulation assays and survival studies

Competitive repopulation assays were performed using BM cells harvested at day +7 from donor C57Bl6 mice ($CD45.2^{+}$) that had been irradiated with 700 cGy TBI and given daily intraperitoneal injections of 0.5 g/G EGF (R&D Systems, Minneapolis, MN) or 200 μl PBS starting at 2 hours post-TBI on day μ 0 through day +7. Competitive repopulation assays were also performed using BM cells from non-irradiated C57Bl6 mice as positive controls to compare with the irradiated/saline treated and irradiated/EGF treated donors. Competitive repopulation assays were also performed with BM harvested at day +14 from donor C57Bl6 mice ($CD45.2^{+}$) that had been irradiated with 700 cGy TBI and gavaged daily with 10 μ g/G erlotinib (Genentech, San Francisco, CA) or 150 μl water beginning on day 0 and continued through day +14. Donor BM cells were injected via tail vein into recipient B6.SJL mice ($CD45.1^{+}$) at a dose of 5×10^5 cells with a competing dose of host 1×10^5 BM MNCs. Primary total $CD45.2^{+}$ donor cell engraftment, multilineage engraftment and donor chimerism within BM KSL cells were measured in recipient mice at 12 weeks post-transplant. Secondary competitive repopulation assays into lethally irradiated B6.SJL mice were performed using 75% of whole BM cells from a group of primary recipient mice, transplanted as described above, and a competing dose of host 1×10^5 BM MNCs. Measurement of donor cell chimerism within the BM KSL population was performed at 12 weeks post-transplantation in primary and secondary transplanted mice, as previously described[16].

Tie2Cre;$Bak1^{-/-}$;$Bax^{fl/-}$ mice were gavaged daily with 10 μg/G erlotinib or water starting day −3 and given 300 cGy TBI on day 0. Erlotinib administration μ continued until the time point of donor BM cell collection and analysis. *Tie2Cre;*$Bak1^{-/-}$;$Bax^{fl/-}$ BM cells were injected via tail vein into recipient $CD45.1^{+}$ mice at a cell dose of 3×10^5 cells with a competing dose of host 1×10^5 $CD45.1^{+}$ cells. Multilineage hematopoietic reconstitution was measured in the PB of recipient mice by flow cytometry at 4, 8, and 12 weeks post-transplant. For survival studies with erlotinib administration, C57Bl6 mice were exposed to 700 cGy and then given 10 μg/G erlotinib or water starting day −3 and continuing daily through day +14. Age matched adult C57Bl6 mice were also exposed to 700 cGy TBI and then given tail vein injections with 0.5 μg/G EGF or saline beginning at +2 hrs post-TBI and then daily through day +7. 700 cGy was chosen for lethality studies because this radiation

dose causes 50% lethality by day +30 in adult C57Bl6 mice at Duke University Medical Center (Cs137 irradiator).

Immunohistochemical analyses

Femurs were decalcified and embedded in OCT media (Sakura Finetek, Torrance, CA) as previously described on days 7 or 14 following 700 cGy TBI with daily administration of EGF or erlotinib. Ten micrometer sections were cut using the CryoJane tape system (Instrumedics Inc, Hackensack, NJ, USA). Femurs were stained with hematoxylin and eosin or anti-mouse endothelial cell antibody (MECA-32) as previously described[4] to assess BM cellularity and the BM vasculature after irradiation. Images were obtained using an Axiovert 200 microscope (Carl Zeiss Microscopy, Thornwood, NY) or a Leica SP5 confocal microscope (Leica Microsystems Inc, Buffalo Grove, IL). Adobe Photoshop software (version 9.0.2, Adobe Systems, San Jose, CA) was used to quantify positive signal as a measure of spatial distribution in the fields[68,69].

Statistical analyses

Data are shown as means ± SEM. We utilized the Mann-Whitney test (two-tailed nonparametric analysis) for the majority of comparisons, along with the Student's t test (two-tailed or one-tailed distribution with unequal variance). Comparisons of overall survival were performed using a Log rank test.

Supplementary Material

Refer to Web version on PubMed Central for supplementary material.

ACKNOWLEDGMENTS

This work was supported in part by NHLBI grant HL-086998-01 (JPC) and NIAID grant AI-067798-06 (JPC) and a pilot project from the NIAID Centers for Medical Countermeasures grant AI-067798-01 (DGK). P.L.D. was supported by NIH training grant, T32 HL0070757-33, the Barton Haynes Award, and Duke Cancer Center Seed Grant (Duke University).

REFERENCES

1. Kiel MJ, Yilmaz OH, Iwashita T, Terhorst C, Morrison SJ. SLAM family receptors distinguish hematopoietic stem and progenitor cells and reveal endothelial niches for stem cells. Cell. 2005; 121:1109–1121. [PubMed: 15989959]
2. Chute JP, Muramoto GG, Fung J, Oxford C. Soluble factors elaborated by human brain endothelial cells induce the concomitant expansion of purified human BM CD34+CD38- cells and SCID-repopulating cells. Blood. 2005; 105:576–583. [PubMed: 15345596]
3. Himburg HA, et al. Pleiotrophin regulates the expansion and regeneration of hematopoietic stem cells. Nat Med. 2010; 16:475–482. [PubMed: 20305662]
4. Salter AB, et al. Endothelial progenitor cell infusion induces hematopoietic stem cell reconstitution in vivo. Blood. 2009; 113:2104–2107. [PubMed: 19141867]
5. Butler JM, et al. Endothelial cells are essential for the self-renewal and repopulation of Notch-dependent hematopoietic stem cells. Cell Stem Cell. 2010; 6:251–264. [PubMed: 20207228]
6. Hooper AT, et al. Engraftment and reconstitution of hematopoiesis is dependent on VEGFR2-mediated regeneration of sinusoidal endothelial cells. Cell Stem Cell. 2009; 4:263–274. [PubMed: 19265665]

7. Montfort MJ, Olivares CR, Mulcahy JM, Fleming WH. Adult blood vessels restore host hematopoiesis following lethal irradiation. Exp Hematol. 2002; 30:950–956. [PubMed: 12160847]
8. Ding L, Saunders TL, Enikolopov G, Morrison SJ. Endothelial and perivascular cells maintain haematopoietic stem cells. Nature. 2012; 481:457–462. [PubMed: 22281595]
9. Chute JP, et al. Ex vivo culture with human brain endothelial cells increases the SCID-repopulating capacity of adult human bone marrow. Blood. 2002; 100:4433–4439. [PubMed: 12393435]
10. Chute JP, Fung J, Muramoto G, Erwin R. Ex vivo culture rescues hematopoietic stem cells with long-term repopulating capacity following harvest from lethally irradiated mice. Exp Hematol. 2004; 32:308–317. [PubMed: 15003317]
11. Muramoto GG, Chen B, Cui X, Chao NJ, Chute JP. Vascular endothelial cells produce soluble factors that mediate the recovery of human hematopoietic stem cells after radiation injury. Biol Blood Marrow Transplant. 2006; 12:530–540. [PubMed: 16635788]
12. Chute JP, et al. Transplantation of vascular endothelial cells mediates the hematopoietic recovery and survival of lethally irradiated mice. Blood. 2007; 109:2365–2372. [PubMed: 17095624]
13. Kirsch DG, et al. p53 controls radiation-induced gastrointestinal syndrome in mice independent of apoptosis. Science. 327:593–596. [PubMed: 20019247]
14. Doan PL, et al. Tie2(+) Bone Marrow Endothelial Cells Regulate Hematopoietic Stem Cell Regeneration Following Radiation Injury. Stem Cells. Nov 6.2012 Epub ahead of print.
15. Yoder MC, et al. Redefining endothelial progenitor cells via clonal analysis and hematopoietic stem/progenitor cell principals. Blood. 2007; 109:1801–1809. [PubMed: 17053059]
16. Guo S, et al. MicroRNA miR-125a controls hematopoietic stem cell number. Proc Natl Acad Sci USA. 2010; 107:14229–14234. [PubMed: 20616003]
17. Boehrer S, et al. Erlotinib exhibits antineoplastic off-target effects in AML and MDS: a preclinical study. Blood. 2008; 111:2170–2180. [PubMed: 17925489]
18. Boehrer S, et al. Erlotinib antagonizes constitutive activation of SRC family kinases and mTOR in acute myeloid leukemia. Cell Cycle. 2011; 10:3168–3175. [PubMed: 21897118]
19. Sordella R, Bell DW, Haber DA, Settleman J. Gefitinib-sensitizing EGFR mutations in lung cancer activate anti-apoptotic pathways. Science. 2004; 305:1163–1167. [PubMed: 15284455]
20. Yang W, et al. Nuclear PKM2 regulates beta-catenin transactivation upon EGFR activation. Nature. 2011; 480:118–122. [PubMed: 22056988]
21. Minder P, Bayha E, Becker-Pauly C, Sterchi EE. Meprinalpha transactivates the epidermal growth factor receptor (EGFR) via ligand shedding, thereby enhancing colorectal cancer cell proliferation and migration. J Biol Chem. 2012; 287:35201–35211. [PubMed: 22923609]
22. Cao C, et al. Galpha(i1) and Galpha(i3) are required for epidermal growth factor-mediated activation of the Akt-mTORC1 pathway. Sci Signal. 2009; 2:ra17. [PubMed: 19401591]
23. Kriegs M, et al. The epidermal growth factor receptor modulates DNA double-strand break repair by regulating non-homologous end-joining. DNA Repair. 2010; 9:889–897. [PubMed: 20615764]
24. Shao L, et al. Deletion of proapoptotic Puma selectively protects hematopoietic stem and progenitor cells against high-dose radiation. Blood. 2010; 115:4707–4714. [PubMed: 20360471]
25. Yu H, et al. Deletion of Puma protects hematopoietic stem cells and confers long-term survival in response to high-dose gamma-irradiation. Blood. 2010; 115:3472–3480. [PubMed: 20177048]
26. Appelbaum FR. Hematopoietic-cell transplantation at 50. N Engl J Med. 2007; 357:1472–1475. [PubMed: 17928594]
27. Chen BJ, et al. Growth hormone mitigates against lethal irradiation and enhances hematologic and immune recovery in mice and nonhuman primates. PloS One. 2010; 5:e11056. [PubMed: 20585403]
28. Waselenko JK, et al. Medical management of the acute radiation syndrome: recommendations of the Strategic National Stockpile Radiation Working Group. Ann Intern Med. 2004; 140:1037–1051. [PubMed: 15197022]
29. Liang Y, Van Zant G, Szilvassy SJ. Effects of aging on the homing and engraftment of murine hematopoietic stem and progenitor cells. Blood. 2005; 106:1479–1487. [PubMed: 15827136]

30. Norddahl GL, et al. Accumulating mitochondrial DNA mutations drive premature hematopoietic aging phenotypes distinct from physiological stem cell aging. Cell Stem Cell. 2011; 8:499–510. [PubMed: 21549326]
31. Elledge SJ. Cell cycle checkpoints: preventing an identity crisis. Science. 1996; 274:1664–1672. [PubMed: 8939848]
32. Levine AJ. p53, the cellular gatekeeper for growth and division. Cell. 1997; 88:323–331. [PubMed: 9039259]
33. Strasser A, Harris AW, Jacks T, Cory S. DNA damage can induce apoptosis in proliferating lymphoid cells via p53-independent mechanisms inhibitable by Bcl-2. Cell. 1994; 79:329–339. [PubMed: 7954799]
34. Quelle FW, et al. Cytokine rescue of p53-dependent apoptosis and cell cycle arrest is mediated by distinct Jak kinase signaling pathways. Genes & development. 1998; 12:1099–1107. [PubMed: 9553040]
35. Herodin F, Bourin P, Mayol JF, Lataillade JJ, Drouet M. Short-term injection of antiapoptotic cytokine combinations soon after lethal gamma -irradiation promotes survival. Blood. 2003; 101:2609–2616. [PubMed: 12468435]
36. Zsebo KM, et al. Radioprotection of mice by recombinant rat stem cell factor. Proc Natl Acad Sci USA. 1992; 89:9464–9468. [PubMed: 1384054]
37. Sinclair WK. Cyclic x-ray responses in mammalian cells in vitro. Radiat Res. 1968; 33:620–643. [PubMed: 4867897]
38. Na Nakorn T, Traver D, Weissman IL, Akashi K. Myeloerythroid-restricted progenitors are sufficient to confer radioprotection and provide the majority of day 8 CFU-S. J Clin Invest. 2002; 109:1579–1585. [PubMed: 12070305]
39. Bill HM, et al. Epidermal growth factor receptor-dependent regulation of integrin-mediated signaling and cell cycle entry in epithelial cells. Mol Cell Biol. 2004; 24:8586–8599. [PubMed: 15367678]
40. Ekert PG, et al. Cell death provoked by loss of interleukin-3 signaling is independent of Bad, Bim, and PI3 kinase, but depends in part on Puma. Blood. 2006; 108:1461–1468. [PubMed: 16705087]
41. Jeffers JR, et al. Puma is an essential mediator of p53-dependent and -independent apoptotic pathways. Cancer Cell. 2003; 4:321–328. [PubMed: 14585359]
42. Coloff JL, et al. Akt requires glucose metabolism to suppress puma expression and prevent apoptosis of leukemic T cells. J Biol Chem. 2011; 286:5921–5933. [PubMed: 21159778]
43. Leibowitz BJ, et al. Uncoupling p53 functions in radiation-induced intestinal damage via PUMA and p21. Mol Cancer Res. 2011; 9:616–625. [PubMed: 21450905]
44. Prigent SA, Gullick WJ. Identification of c-erbB-3 binding sites for phosphatidylinositol 3′-kinase and SHC using an EGF receptor/c-erbB-3 chimera. EMBO J. 1994; 13:2831–2841. [PubMed: 8026468]
45. Dittmann K, et al. Radiation-induced epidermal growth factor receptor nuclear import is linked to activation of DNA-dependent protein kinase. J Biol Chem. 2005; 280:31182–31189. [PubMed: 16000298]
46. Rodemann HP, Dittmann K, Toulany M. Radiation-induced EGFR-signaling and control of DNA-damage repair. Int J Radiat Biol. 2007; 83:781–791. [PubMed: 18058366]
47. Cardo-Vila M, et al. From combinatorial peptide selection to drug prototype (II): targeting the epidermal growth factor receptor pathway. Proc Natl Acad Sci USA. 2010; 107:5118–5123. [PubMed: 20190183]
48. Ji H, et al. The impact of human EGFR kinase domain mutations on lung tumorigenesis and in vivo sensitivity to EGFR-targeted therapies. Cancer Cell. 2006; 9:485–495. [PubMed: 16730237]
49. Aguirre A, Rubio ME, Gallo V. Notch and EGFR pathway interaction regulates neural stem cell number and self-renewal. Nature. 2010; 467:323–327. [PubMed: 20844536]
50. Natarajan A, Wagner B, Sibilia M. The EGF receptor is required for efficient liver regeneration. Proc Natl Acad Sci USA. 2007; 104:17081–17086. [PubMed: 17940036]
51. Shih CC, et al. Identification of a candidate human neurohematopoietic stem-cell population. Blood. 2001; 98:2412–2422. [PubMed: 11588038]

52. Pain B, et al. EGF-R as a hemopoietic growth factor receptor: the c-erbB product is present in chicken erythrocytic progenitors and controls their self-renewal. Cell. 1991; 65:37–46. [PubMed: 1672832]
53. von Ruden T, Wagner EF. Expression of functional human EGF receptor on murine bone marrow cells. EMBO J. 1988; 7:2749–2756. [PubMed: 3053164]
54. Takahashi T, et al. A potential molecular approach to ex vivo hematopoietic expansion with recombinant epidermal growth factor receptor-expressing adenovirus vector. Blood. 1998; 91:4509–4515. [PubMed: 9616146]
55. Ryan MA, et al. Pharmacological inhibition of EGFR signaling enhances G-CSF-induced hematopoietic stem cell mobilization. Nat Med. 2010; 16:1141–1146. [PubMed: 20871610]
56. Chan G, Nogalski MT, Yurochko AD. Activation of EGFR on monocytes is required for human cytomegalovirus entry and mediates cellular motility. Proc Natl Acad Sci USA. 2009; 106:22369–22374. [PubMed: 20018733]
57. Dooley DC, et al. Basic fibroblast growth factor and epidermal growth factor downmodulate the growth of hematopoietic cells in long-term stromal cultures. J Cell Physiol. 1995; 165:386–397. [PubMed: 7593217]
58. Zhang CC, Lodish HF. Murine hematopoietic stem cells change their surface phenotype during ex vivo expansion. Blood. 2005; 105:4314–4320. [PubMed: 15701724]
59. Hashimoto M, et al. Fibroblast growth factor 1 regulates signaling via the glycogen synthase kinase-3beta pathway. Implications for neuroprotection. J Biol Chem. 2002; 277:32985–32991. [PubMed: 12095987]
60. Shen H, et al. An acute negative bystander effect of gamma-irradiated recipients on transplanted hematopoietic stem cells. Blood. 2012; 119:3629–3637. [PubMed: 22374698]

METHODS REFERENCES

61. Lee TC, Threadgill DW. Generation and validation of mice carrying a conditional allele of the epidermal growth factor receptor. Genesis. 2009; 47:85–92. [PubMed: 19115345]
62. Georgiades P, et al. VavCre transgenic mice: a tool for mutagenesis in hematopoietic and endothelial lineages. Genesis. 2002; 34:251–256. [PubMed: 12434335]
63. de Boer J, et al. Transgenic mice with hematopoietic and lymphoid specific expression of Cre. Eur J Immunol. 2003; 33:314–325. [PubMed: 12548562]
64. Till JE, Mc CE. A direct measurement of the radiation sensitivity of normal mouse bone marrow cells. Radiat Res. 1961; 14:213–222. [PubMed: 13776896]
65. Jordan CT, Yamasaki G, Minamoto D. High-resolution cell cycle analysis of defined phenotypic subsets within primitive human hematopoietic cell populations. Exp Hematol. 1996; 24:1347–1355. [PubMed: 8862447]
66. Chute JP, et al. Preincubation with endothelial cell monolayers increases gene transfer efficiency into human bone marrow CD34(+)CD38(-) progenitor cells. Hum Gene Ther. 2000; 11:2515–2528. [PubMed: 11119422]
67. Bungartz G, Land H, Scadden DT, Emerson SG. NF-Y is necessary for hematopoietic stem cell (HSC) proliferation and survival. Blood. 2011; 119:1380–1389. [PubMed: 22072554]
68. Lehr HA, Mankoff DA, Corwin D, Santeusanio G, Gown AM. Application of photoshop-based image analysis to quantification of hormone receptor expression in breast cancer. J Histochem Cytochem. 1997; 45:1559–1565. [PubMed: 9358857]
69. Lehr HA, van der Loos CM, Teeling P, Gown AM. Complete chromogen separation and analysis in double immunohistochemical stains using Photoshop-based image analysis. J Histochem Cytochem. 1999; 47:119–126. [PubMed: 9857219]

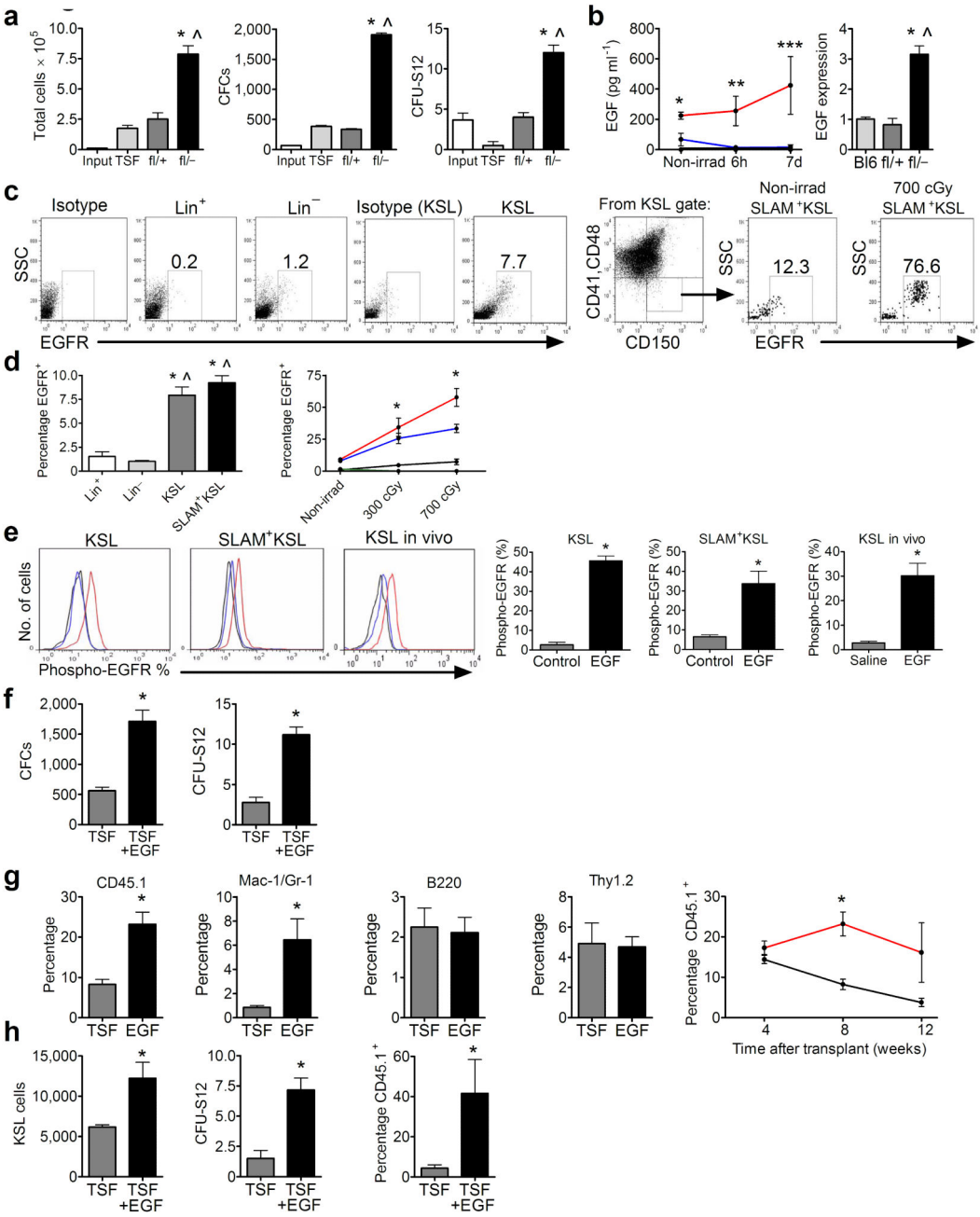

Figure 1.

Tie2^{+} BM ECs produce EGF and EGF mediates HSC regeneration following irradiation. (**a**) Mean numbers (±SEM) of total cells (left), CFCs (middle) and CFU-S12 (right) are shown at day +7 from non-contact cultures of 300 cGy-irradiated BM KSL cells with BM ECs from *Tie2Cre;Bak1*$^{-/-}$*;Bax*$^{fl/-}$ mice (fl/-) compared to culture with BM ECs from *Tie2Cre;Bak1*$^{-/-}$*;Bax*$^{fl/+}$ mice (fl/+) or cytokines alone (TSF). **P*=0.003 and ^*P*=0.04 versus TSF and fl/+, respectively, for total cells (*n*=3-7/condition); **P*<0.0001 and ^*P*<0.0001 versus TSF and fl/+, respectively, for CFCs (*n*=3/condition, t-test); **P*=0.04 and

^*P*=0.02 versus TSF and fl/+, respectively, for CFU-S12 (*n*=3-5/condition). (**b**) At left, concentrations of EGF are shown in the BM serum of *Tie2Cre;Bak1*$^{-/-}$*;Bax*$^{fl/-}$ mice (red line), *Tie2Cre;Bak1*$^{-/-}$*;Bax*$^{fl/+}$ mice (blue line) and C57Bl6 mice (black line) prior to irradiation and at 6 hrs and 7 days post-750 cGy. **P*=0.02, ***P*=0.04, ****P*=0.04 vs *Tie2Cre;Bak1*$^{-/-}$*;Bax*$^{fl/+}$ mice, *n*=3/condition, means ± SEM, 1-tailed t-test. At right, EGF expression is shown in fl/− ECs (fl/-), fl/+ ECs (fl/+) and C57Bl6 ECs (Bl6) by qRT-PCR. **P*=0.002 and ^*P*=0.003 vs. Bl6 ECs and fl/+ ECs, means ± SEM (n=3/group, 2-tailed t-test). (**c**) At left, representative EGFR surface expression is shown on BM lin$^+$ cells, lin$^-$ cells, and KSL cells from C57Bl6 mice. At right, representative EGFR surface expression is shown on non-irradiated BM SLAM$^+$KSL cells and at 4 hours following 700 cGy. (**d**) At left, EGFR surface expression on each BM subset is shown. **P*=0.009 and ^*P*<0.001 for BM KSL cells vs. BM lin$^+$ and lin$^-$ cells, respectively. **P*=0.02 and ^*P*=0.004 for BM SLAM$^+$KSL cells vs. lin$^+$ cells and lin$^-$ cells, respectively (*n*=3-9/group, means ± SEM). At right, EGFR expression on non-irradiated BM SLAM$^+$KSL cells (red line), KSL cells (blue line), lin$^-$ cells (black line) and lin$^+$ cells (green line) and at 4 hours following 300 cGy and 700 cGy TBI. **P*=0.002 for difference in SLAM$^+$KSL cells between 300 cGy and non-irradiated group, **P*=0.001 for difference between 700 cGy and non-irradiated group (*n*=3-7/group, means ± SEM). (**e**) Representative FACS analyses of EGFR-phosphorylation of Tyr-1173 in BM KSL cells (left) and BM SLAM$^+$KSL cells (middle) in serum free culture (blue curve) or in same conditions plus EGF (red curve). At right, EGFR-phosphorylation is shown in BM KSL cells in mice treated with EGF (red curve) or saline (blue). Isotype stained cells are shown in black. Levels of EGFR-phosphorylation are shown for each group at right. **P*=0.008 for EGF vs. control cultures of KSL cells, **P*<0.001 for EGF vs. control cultures of BM SLAM$^+$KSL cells (*n*=5/group, means ± SEM), **P*=0.03 for EGF vs. saline treatment, KSL cells in vivo (*n*=4/group). (**f**) CFC and CFU-S12 content of cultures of irradiated BM KSL cells with TSF or TSF + EGF are shown; **P*=0.0002 and **P*=0.0003, respectively, for CFCs (*n*=8/group) and CFU-S12 (*n*=9-12/group) versus TSF alone; means ± SEM. (**g**) PB donor CD45.1$^+$ cell, myeloid (Mac-1/Gr-1), B cell (B220) and T cell (Thy1.2) engraftment at 8 weeks post-transplant in CD45.2$^+$ mice following transplantation of irradiated/TSF-cultured 34$^-$KSL cells or irradiated/TSF+EGF-cultured 34$^-$KSL cells (*n*=7-9/group). **P*=0.002 for CD45.1$^+$ engraftment and **P*=0.002 for myeloid engraftment. Total PB CD45.1$^+$ cell engraftment over time is shown at right (red line=TSF +EGF culture, black line=TSF alone). **P*=0.002 (means ± SEM). (**h**) Numbers of KSL cells and CFU-S12 are shown from cultures of BM KSL cells with TSF or TSF + EGF. **P*=0.03 and **P*=0.004, (means ± SEM, *n*=4-6/group). At right, percent donor CD45.1$^+$ cell engraftment at 12 weeks is shown in mice that were transplanted with non-irradiated/TSF-cultured 34$^-$KSL cells or non-irradiated/TSF+EGF-cultured 34$^-$KSL cells. **P*=0.04 (means ± SEM, *n*=4-5 mice/group, 2-tailed t test). The Mann-Whitney test was used for all analyses unless otherwise noted.

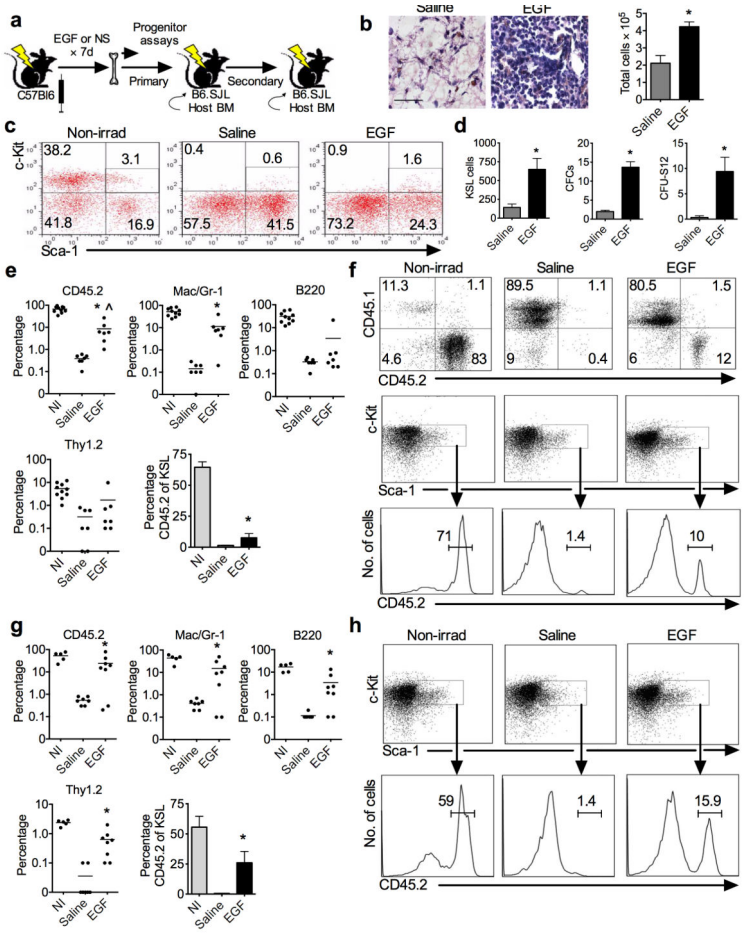

Figure 2.

Systemic administration of EGF promotes HSC regeneration in vivo. (**a**) Schematic diagram of treatment of mice following TBI with either EGF or normal saline (NS) IP x 7 days and subsequent analysis of BM progenitor cell content and competitive HSC repopulation assays. (**b**) Representative H&E stained femurs from EGF-treated and saline-treated mice are shown (scale bar 250 microns). BM cell counts are shown at right. **P*=0.003 (means ± SEM, *n*=6/group). (**c**) Representative FACS analysis of BM c-kit$^+$sca-1$^+$ cells within the lin $^-$ gate (KSL) from non-irradiated mice and at day +7 from irradiated/saline-treated or irradiated/EGF-treated mice. (**d**) BM KSL cells, CFCs and CFU-S12 at day +7 in irradiated/saline-treated and irradiated/EGF-treated mice. **P*=0.008 for KSL cells (means ± SEM, *n*=6/group), **P*<0.0001 and **P*=0.03 for CFCs and CFU-S12 (means ± SEM, *n*=3-5/group). (**e**) Percent total donor CD45.2$^+$ cell, myeloid (Mac-1), B cell (B220) and T cell (Thy 1.2) engraftment is shown in the BM of CD45.1$^+$ mice at 12 weeks following transplantation of 5 × 10^5 BM cells from non-irradiated donor mice (NI), irradiated/saline-treated mice or irradiated/EGF-treated mice. **P*=0.0006 for EGF vs. saline, ^*P*=0.0001 for EGF vs. NI (CD45.2$^+$ engraftment), **P*=0.002 for EGF vs. saline (myeloid engraftment)(*n*=7-10/group, Mann-Whitney). Horizontal lines represent mean levels of donor cell engraftment. Levels of donor CD45.2$^+$ cells within the BM KSL population are also shown. **P*=0.001 and ^*P*=0.0001 for EGF vs. saline and NI group, respectively (*n*=7-10/group, means ± SEM). (**f**)

Representative FACS plots are shown of total donor CD45.2$^+$ cells and CD45.2$^+$ cell chimerism within BM KSL cells at 12 weeks in mice transplanted with BM from NI mice, irradiated/saline-treated mice or irradiated/EGF-treated mice. (**g**) Percent donor CD45.2$^+$ cell, myeloid, B cell and T cell engraftment is shown at 12 weeks in the BM of secondary transplant recipient mice (CD45.1$^+$) in the NI group, irradiated/saline-treatment group and the irradiated/EGF-treatment group. **P*=0.03, **P*=0.04, **P*=0.02, **P*=0.001 for differences in total CD45.2$^+$ cell engraftment, myeloid cell, B cell and T cell engraftment, respectively, between EGF vs. saline groups (*n*=5-8/group, means ± SEM). The mean levels of donor CD45.2$^+$ cells within the BM KSL population are also shown. **P*=0.009 for EGF vs. saline group (*n*=5-8/group, means ± SEM). (**h**) Representative FACS plots are shown of CD45.2$^+$ cell chimerism within BM KSL cells in secondary transplanted mice in the NI, saline- and EGF-treatment groups at 12 weeks post-transplantation.

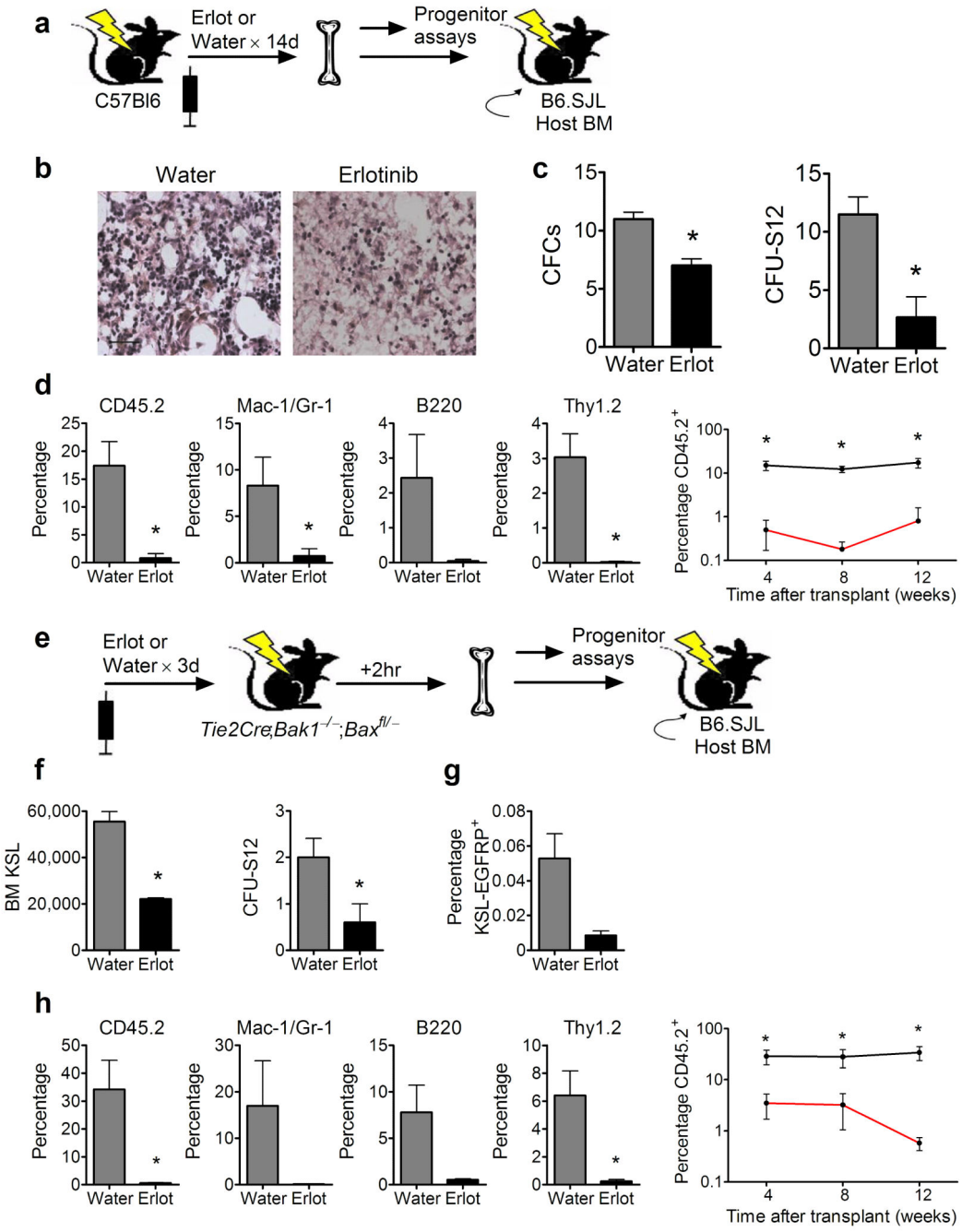

Figure 3.

Erlotinib treatment inhibits HSC regeneration in vivo following TBI (**a**) Schematic diagram of TBI and erlotinib treatment of C57Bl6 mice, with evaluation of BM progenitor cells and HSC repopulating capacity at day +14. (**b**) BM cellularity is shown at day +14 in the erlotinib and water treatment groups (scale bar 250 microns). (**c**) BM CFCs (per 2×10^4 cells) and BM CFU-S12 are shown in erlotinib-treated and water-treated mice at day +14. **P*=0.008 and **P*=0.04 (means ± SEM, *n*=3/group). (**d**) Percent donor $CD45.2^+$ cell, Mac-1/Gr-1, B220 and Thy1.2 cell engraftment is shown in the PB of $CD45.1^+$ mice at 12 weeks

following competitive transplantation of 5×10^5 BM cells from irradiated/erlotinib-treated mice or irradiated/water-treated controls (*n*=3-4/group, means ± SEM). **P*=0.007 for total CD45.2$^+$ cell engraftment. **P*=0.04 and **P*=0.003 for myeloid cell and T cell differences, respectively. At right, PB donor cell engraftment over time is shown in mice transplanted with BM from irradiated/erlotinib-treated donors (red line) and irradiated/water-treated donors (black line). **P*=0.002, **P*=0.0002, and **P*=0.007 at 4, 8, and 12 weeks, respectively (*n*=3-4/group). (**e**) Schematic diagram of irradiation and treatment of *Tie2Cre;Bak1*$^{-/-}$*;Bax*$^{fl/-}$ mice with erlotinib or water. (**f**) BM KSL cells and CFU-S12 content at +2 hours post-TBI in erlotib-treated and water-treated mice. **P*=0.02 and **P*=0.046 for BM KSL and CFU-S12, respectively (*n*=2-5, means ± SEM). (**g**) The percentage of BM KSL cells with EGFR phosphorylation in erlotinib-treated and water-treated mice is shown (*n*=2, means ± SEM). (**h**) Percent donor CD45.2$^+$ cell, Mac-1/Gr-1, B220 and Thy1.2 cell engraftment in CD45.1$^+$ mice is shown at 12 weeks following competitive transplant of 3×10^5 BM cells from erlotinib-treated or water-treated mice. **P*=0.03 and **P*=0.02 for CD45.2$^+$ cell and T-cell engraftment (means ± SEM, *n*=4-6/group, top). Donor CD45.2$^+$ cell engraftment is shown over time in mice transplanted with BM cells from erlotinib-treated mice (red line) or water-treated mice (black line). **P*=0.009, **P*<0.0001 and **P*=0.03 for differences at 4 weeks, 8 weeks and 12 weeks, respectively (bottom). A 2-tailed t-test was used for all analyses.

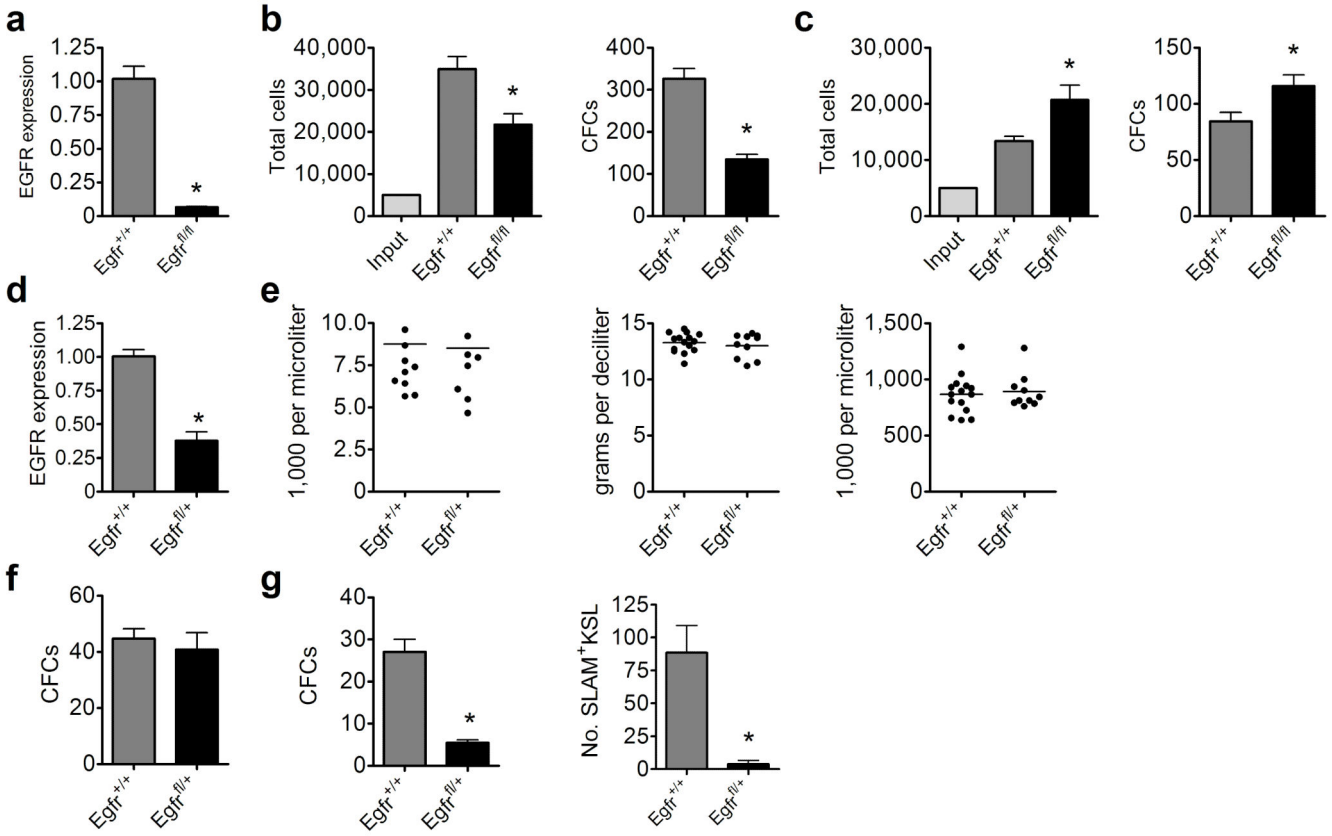

Figure 4.

Deletion of EGFR inhibits hematopoietic progenitor cell regeneration. (**a**) EGFR gene expression is shown in BM lin$^-$ cells from *VavCre;EGFR$^{fl/fl}$* mice and *VavCre;EGFR$^{+/+}$* mice. **P*=0.008 (means ± SEM, *n*=5/group). (**b**) The numbers of total cells and CFCs at 72 hours of cytokine culture of BM lin$^-$ cells from *VavCre;EGFR$^{fl/fl}$* mice and *VavCre;EGFR$^{+/+}$* mice are shown. **P*=0.03 and **P*=0.002 for total cells and CFCs, respectively (means ± SEM, *n*=5-6/group). (**c**) Numbers of total cells and CFCs are shown at 72 hours of culture of BM KSL cells from *VavCre;EGFR$^{fl/fl}$* mice and *VavCre;EGFR$^{+/+}$* mice with erlotinib. **P*=0.004 and **P*=0.04 for total cells and CFCs, respectively (*n*=8/group). (**d**) EGFR expression in BM lin$^-$ cells from *VavCre;EGFR$^{fl/+}$* mice and *VavCre;EGFR$^{+/+}$* mice. **P*=0.008 (means ± SEM, *n*=5/group. (**e**) Complete blood counts (*n*=10-15/group) and (**f**) BM CFCs are shown in *VavCre;EGFR$^{+/+}$* mice and *VavCre;EGFR$^{fl/+}$* mice (*n*=6/group). (**g**) Numbers of BM CFCs and BM SLAM$^+$KSL cells are shown in *VavCre;EGFR$^{fl/+}$* mice and *VavCre;EGFR$^{+/+}$* mice at day +7 following 500 cGy TBI. **P*=0.002 (*n*=6/group) and **P*=0.004 (*n*=6-11/group) for CFCs and SLAM$^+$KSL cells, respectively. The Mann-Whitney test was applied for all analyses.

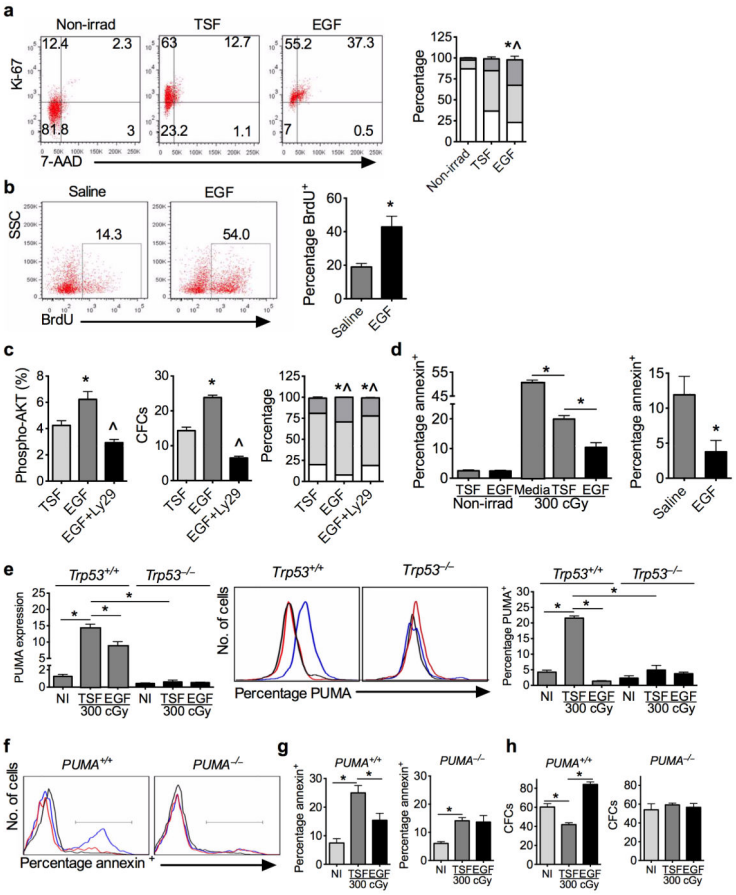

Figure 5.

EGF promotes HSC cycling and survival following irradiation. (**a**) Representative FACS analysis of cell cycle status of BM KSL cells at day 0 and 72 hrs following irradiation/TSF culture or irradiation/TSF + EGF culture. G_0 = white bar, G_1 = light gray bar, G_2/S/M = gray bar. **P*=0.002 and ^*P*=0.002 vs. TSF for G_0 and G_2/S/M (means ± SEM, *n*=3-5). (**b**) Representative BrdU incorporation in BM KSL cells in vivo at day + 7 following 700 cGy TBI and treatment with EGF or saline (left); mean BrdU incorporation shown at right; **P*=0.02 (means ± SEM, *n*=3/group, 2-tailed t-test). (**c**) At left, %phospho-AKT levels in BM KSL cells following 300 cGy and the culture conditions shown. **P*=0.03 TSF vs. EGF, ^*P*=0.0006 EGF vs. EGF + Ly29 (means ± SEM, *n*=7-8/group). Middle, CFCs at 72 hrs after 300 cGy in the culture conditions shown. **P*=0.002, TSF vs. EGF; ^*P*=0.002 EGF vs. EGF+Ly29 (means ± SEM, *n*=6 /group). At right, cell cycle status of KSL cells at 72 hrs after 300 cGy in the culture conditions shown. White bar = G_0, light gray bar = G_1, gray bar = G_2/S/M phase. EGF vs. TSF: **P*<0.0001 for G_0, ^*P*=0.004 for G_2/S/M; EGF + Ly29 vs. EGF: **P*<0.0001 for G_0, ^*P*=0.0001 for G_2/S/M; *n*=4-5/group, means ± SEM, 2-tailed t test. (**d**) At left, %Annexin$^+$ BM KSL cells are shown at 72 hrs of culture with TSF or TSF + EGF and after 300 cGy and the culture conditions shown. **P*=0.002 for EGF vs. TSF; **P*=0.004 for media vs. TSF (means ± SEM, *n*=4-8/group). At right, %Annexin$^+$ CD45$^+$MECA$^-$ cells in the BM at day +7 following 700 cGy TBI and treatment with saline or EGF. **P*=0.03 (means ± SEM, *n*=4-5/group, right). (**e**) At left, PUMA gene expression is

shown in BM KSL cells from $p53^{+/+}$ mice and $p53^{-/-}$ mice at 6 hrs in the conditions shown. NI = non-irradiated control. **P*=0.01 for NI vs. irradiated/TSF, **P*=0.03 for EGF vs. TSF, **P*=0.03 for TSF ($p53^{+/+}$) vs. TSF ($p53^{-/-}$)(*n*=4-6/group, means ± SEM). At middle, representative FACS analyses of PUMA protein levels in irradiated/TSF-cultured KSL cells (blue line), irradiated/TSF+EGF-cultured KSL cells (red line) and non-irradiated BM KSL cells (black line) from $p53^{+/+}$ and $p53^{-/-}$ mice. At right, mean percentages of PUMA protein levels in KSL cells from $p53^{+/+}$ and $p53^{-/-}$ mice in the culture conditions described above. **P*<0.001 for NI vs. irradiated/TSF group, **P*=0.01 for EGF vs. TSF group, **P*<0.001 for TSF ($p53^{+/+}$) vs. TSF ($p53^{-/-}$) (*n*=3/group, means + SEM, 2-tailed t-test). (**f**) Representative FACS plot of %$Annexin^{+}$ BM KSL cells from $PUMA^{+/+}$ mice and $PUMA^{-/-}$ mice at 72 hours in irradiated/TSF cultures (blue lines), irradiated/TSF+EGF cultures (red line) and non-irradiated BM KSL cells (black line). (**g**) Mean %$Annexin^{+}$ BM KSL cells from $PUMA^{+/+}$ mice and $PUMA^{-/-}$ mice at 72 hrs in the groups shown. **P*=0.002 for NI vs. irradiated/TSF ($PUMA^{+/+}$), **P*=0.02 for EGF vs. TSF ($PUMA^{+/+}$), **P*=0.003 for NI vs. irradiated/TSF ($PUMA^{-/-}$). Note: *P*=0.002 for TSF ($PUMA^{+/+}$) vs. TSF ($PUMA^{-/-}$)(*n*=4-9/group, means ± SEM). (**h**) CFCs from BM KSL cells from $PUMA^{+/+}$ mice and $PUMA^{-/-}$ mice in the irradiated/TSF-culture and irradiated/TSF+EGF culture groups. **P*=0.006 for NI vs. irradiated/TSF ($PUMA^{+/+}$), **P*=0.001 for EGF vs. TSF ($PUMA^{+/+}$). Note: *P*=0.02 for TSF ($PUMA^{+/+}$) vs. TSF ($PUMA^{-/-}$)(*n*=6/group, means + SEM). The Mann-Whitney test was utilized.

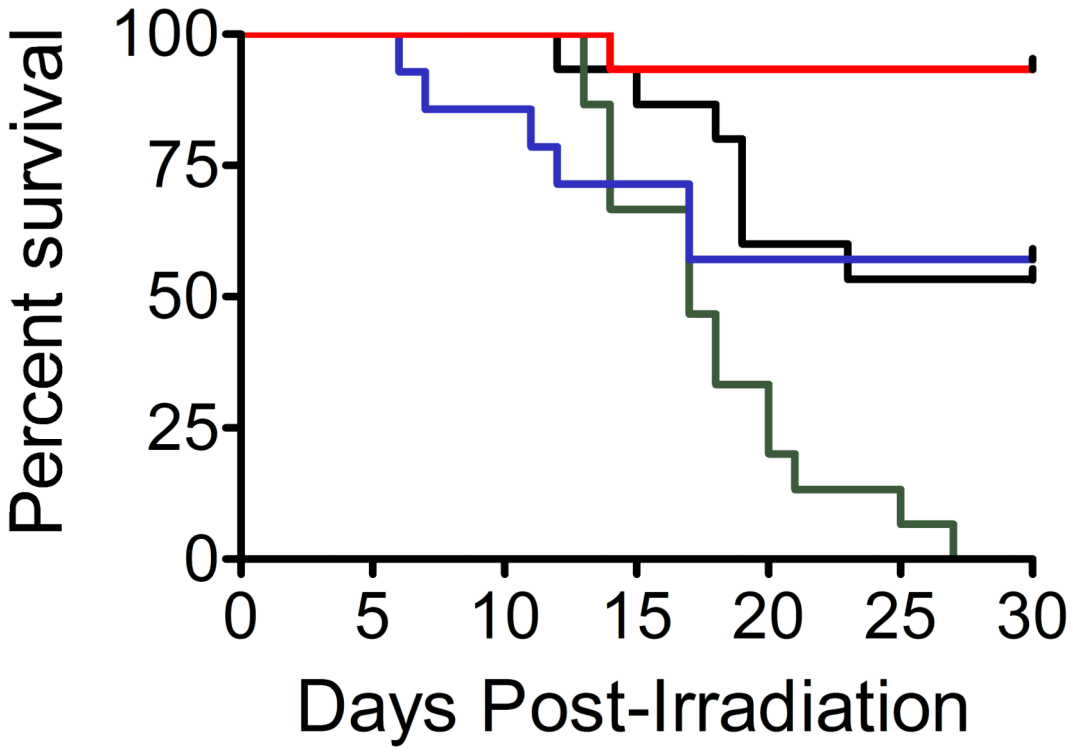

Figure 6.

Pharmacologic modulation of EGFR signaling alters mice survival following TBI. The survival curves are shown of C57Bl6 mice that were irradiated with 700 cGy TBI followed by daily EGF (red curve) or saline treatments (blue curve) for 7 days. **P*=0.02 for EGF vs. saline survival. The survival curves of C57Bl6 mice irradiated with 700 cGy TBI and treated with 10 μg/g erlotinib (green curve) or water (black curve) from day −3 to day +14 are also shown. **P*=0.003 for erlotinib vs. water survival. Log rank test was utilized for comparisons.